Electronic Supplementary Material (ESI) for Journal of Materials Chemistry A


# Electronic supplementary information (ESI)

## High Energy and Power Density $TiO_2$ Nanotube Electrodes for 3D Li-ion Microbatteries

Wei Wei*[a], Gabriel Oltean[a], Cheuk-Wai Tai[b], Kristina Edström[a], Fredrik Björefors[a] and Leif Nyholm[a]

*a Department of Chemistry - Ångström Laboratory, Uppsala University*
*Box 538, SE-751 21 Uppsala, Sweden*
*b Department of Materials and Environmental Chemistry, Stockholm University*
*SE-106 91 Stockholm, Sweden*

* Corresponding author
E-mail: wei.wei@kemi.uu.se (Dr. W.Wei)

### S1 Anodic formation of self-organized oxide nanotubes

Self-organized oxide tube arrays or pore arrays can be obtained by an anodization process involving some transition metals, such as Ti, Nb, Ta, Zr. When these metals are exposed to a sufficiently high anodic potential in an electrochemical cell (as that shown in Figure S1a), an oxidation reaction (i)

$$M + x\,H_2O \rightarrow MO_x + 2x\,H^+ + 2x\,e^- \qquad \text{(i)}$$

will be initiated and an oxide layer will form on the metal substrate. If fluoride ions are added to the electrolyte, a competing chemical dissolution reaction (ii) will be established (as illustrated in Figure S1b).

$$MO_x + y\,F^- + 2x\,H^+ \rightarrow [MF_y]^{2x-y} + x\,H_2O \qquad \text{(ii)}$$

The initial stage (stage I in Figure S1c) of the oxide nanotube formation is the growth of a compact oxide layer on the metal substrate (see reaction (i)). Due to the random chemical etching by fluoride ions, irregular tiny pores are then formed which penetrate the initial compact oxide (see stage II in Figure S1c). Due to the competition between oxide formation and chemical dissolution at the different interfaces, a more ordered oxide nanotube/nanopore layer starts to form and continuously grows into the metal substrate (see stage III in Figure S1c). .[1] The initial layer with some irregular pore/tube often remains as remnants on the nanotube tops, as shown in Figure S2a and S2b.

The two-step anodization approach employed in this work is an effective method to form highly self-ordered $TiO_2$ nanotubes with well-defined top morphologies.[2] In this process, the relative long-term anodization during the first step yield $TiO_2$ nanotubes and an underlying textured substrate with an arrangement of self-ordered dimples. By strong sonication in deionized water, the formed $TiO_2$ nanotubes can be detached and the textured substrate exposed. In the second anodization step, highly self-ordered $TiO_2$ nanotube arrays with a well-defined nano-ring top layer can be grown based in the dimples arrangement on the substrate resulting from the initial anodization step.

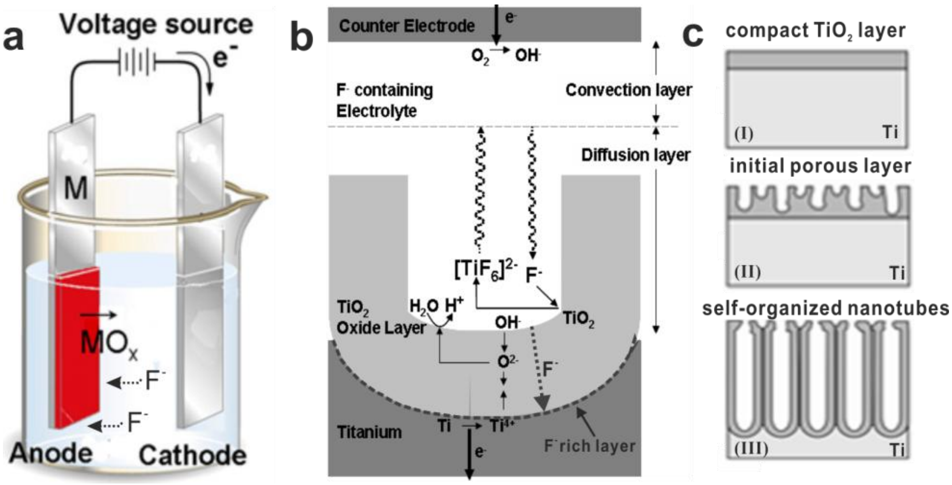


**Figure S1**. (a) Schematic set-up for anodization experiments. (b) Schematic representation of the anodization of Ti in fluoride containing electrolytes. (c) Schematic representation of the typical sequence of anodic tube formation.[1]

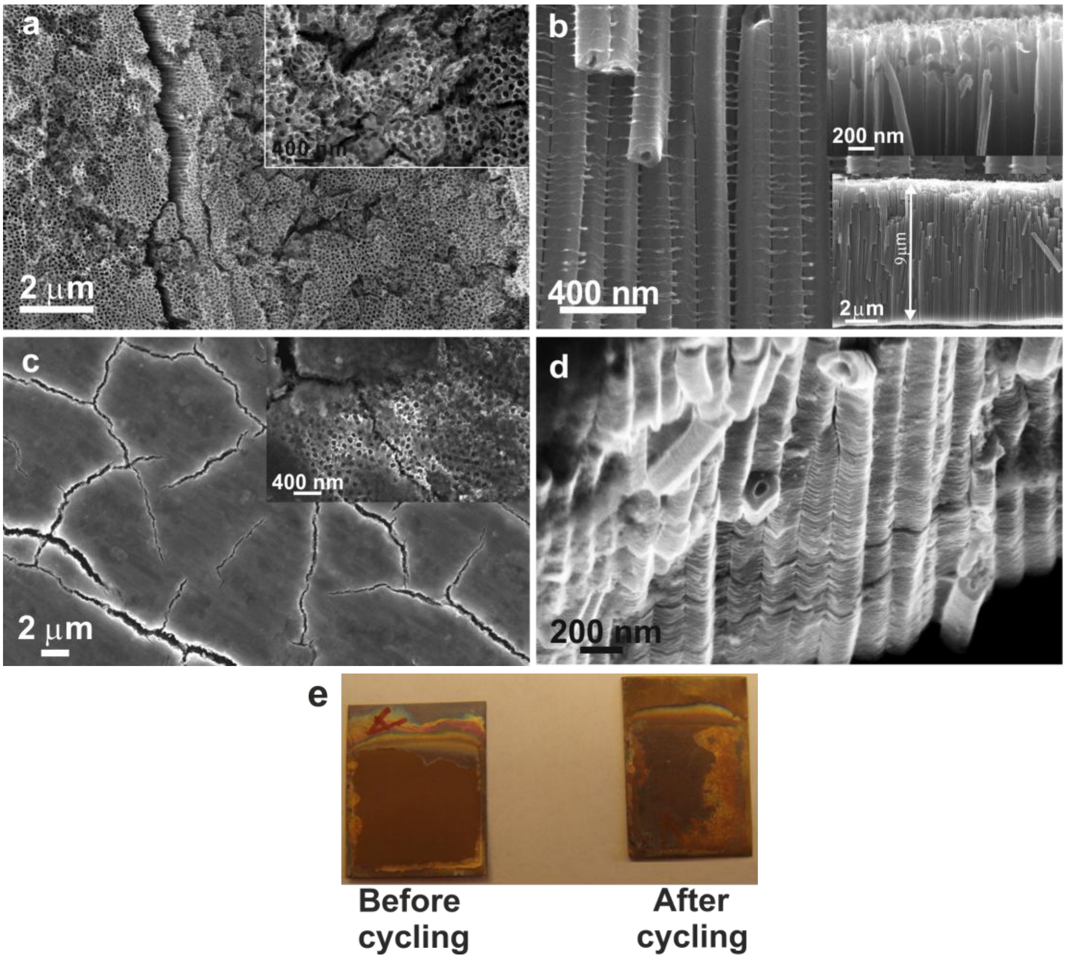


**Figure S2.** SEM micrograph of annealed, one-step anodized $TiO_2$ nanotube electrode (a) and (b) before and (c) and (d) after battery cycling tests, showing (a) and (c) top-views and (b) and (d) cross-sectional views. The insets in (a) and (c) show high magnification top-views whereas in (b) show a cross-sectional view at tube top and the tube lengths. (e) Optical images of the $TiO_2$ nanotube electrodes before (left) and after (right) battery cycling.

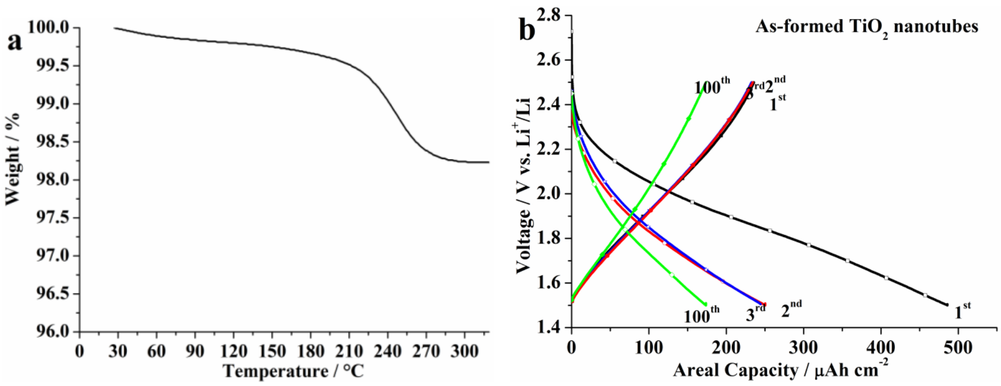


**Figure S3**. (a) Thermogravimetric analysis (TGA) curve for an as-prepared $TiO_2$ nanotube electrode. **(**b) Charge and discharge curves for the 1$^{st}$, 2$^{nd}$, 3$^{rd}$ and 100$^{th}$ cycles for the as-prepared, two-step anodized $TiO_2$ nanotube electrode, recorded at a rate of C/10.

**Table S4**. Comparison of the performance of the present anatase nanotube electrode based cell with those of other microbattery systems

| Ref. | Active material | Areal capacity at low rate | cycling stablity* | Areal Capacity at high rate |
|---|---|---|---|---|
| **Our Result** | **$TiO_2$ nanotube electrode** | **465 μAh $cm^{-2}$ at 50 μA $cm^{-2}$** | **94% after 500 cycles** | **222 μAh $cm^{-2}$ at 2.5 mA $cm^{-2}$** |
| [3] | Li/LiPON/$LiCoO_2$ 2D thin-film | 133 μAh $cm^{-2}$ at 33 μA $cm^{-2}$ | capacity was stable over 100 cycles | 120 μAh $cm^{-2}$ at 0.333 mA $cm^{-2}$ |
| [4] | LiCx/PVDF/$MoO_yS_z$ 3D structures | ~1000 μAh $cm^{-2}$ at 200 μA $cm^{-2}$ | 60% after 200 cycles | 600 μAh $cm^{-2}$ at 2 mA $cm^{-2}$ |
| [5] | $Fe_3O_4$ nanoarchitectures | 340 μAh $cm^{-2}$ at 23 μA $cm^{-2}$ | "capacity was sustained over 100 cycles" | 260 μAh $cm^{-2}$ at 2.9 mA $cm^{-2}$ |
| [6] | $TiO_2$ 2D thin-film | 13 μAh $cm^{-2}$ at 2.6 μA $cm^{-2}$ | unkown | 6.6 μAh $cm^{-2}$ at 0.33 mA $cm^{-2}$ |
| [7] | PPYDBS/carbon microarrays | 35.1 μAh $cm^{-2}$ at 7 μA $cm^{-2}$ | unknown | 31.6 μAh $cm^{-2}$ at 0.07 mA $cm^{-2}$ |
| [8] | $TiO_2$ nanoarchitectures | 11.2 μAh $cm^{-2}$ at 1 μA $cm^{-2}$ | 85% after 50 cycles | 3.92 μAh $cm^{-2}$ at 0.1 mA $cm^{-2}$ |
| [9] | $TiO_2$ nanotube electrode | 77 μAh $cm^{-2}$ at 5 μA $cm^{-2}$ | 71% after 50 cycles | 33 μAh $cm^{-2}$ at 0.1 mA $cm^{-2}$ |
| [10] | $TiO_2$ nanotube electrode | 40 μAh $cm^{-2}$ at 173 μA $cm^{-2}$ | 95.7% after 100 cycles | 21 μAh $cm^{-2}$ at 8.6 mA $cm^{-2}$ |
| [11] | $LiCoO_2$ nanoarchitectures | 120 μAh $cm^{-2}$ at 12 μA $cm^{-2}$ | 88% after 65 cycles | 81.6 μAh $cm^{-2}$ at 0.96 mA $cm^{-2}$ |
| [12] | $Fe_2O_3$ nanowire /$TiO_2$ nanotube | 240 μAh $cm^{-2}$ at 12.5 μA $cm^{-2}$ | 50% after 45 cycles | 60 μAh $cm^{-2}$ at 0.05 mA $cm^{-2}$ |
| [13] | SnO nanowire / $TiO_2$ nanotube | 119 μAh $cm^{-2}$ at 50 μA $cm^{-2}$ | 85% after 50 cycles | 66.5 μAh $cm^{-2}$ at 0.1 mA $cm^{-2}$ |
| [14] | PMMA-PEO / $TiO_2$ nanotube | 119 μAh $cm^{-2}$ at 5 μA $cm^{-2}$ | 93% after 50 cycles | 50 μAh $cm^{-2}$ at 0.025 mA $cm^{-2}$ |
| [15] | $TiO_2$ Nanowire Network | 170 μAh $cm^{-2}$ at 16 μA $cm^{-2}$ | 100% after 600 cycles | 60 μAh $cm^{-2}$ at 0.8 mA $cm^{-2}$ |
| [16] | $SnO_2$/α- $Fe_2O_3$ nanotube array | 344 μAh $cm^{-2}$ at 300 μA $cm^{-2}$ | 85% after 50 cycles | unknown |
| [17] | $TiO_2$ nanotube electrode | 136 μAh $cm^{-2}$ at 100 μA $cm^{-2}$ | 93% after 100 cycles | 120 μAh $cm^{-2}$ at 1 mA $cm^{-2}$ |
| [18] | $V_2O_5$ nanocoating | 37 μAh $cm^{-2}$ at 9 μA $cm^{-2}$ | 100% after 35 cycles | 25 μAh $cm^{-2}$ at 0.09 mA $cm^{-2}$ |
| [19] | $LiFePO_4$/RVC electrodes | 325 μAh $cm^{-2}$ at 65 μA $cm^{-2}$ | 98% after 43 cycles | 225 μAh $cm^{-2}$ at 1.5 mA $cm^{-2}$ |

* Capacity remaining after x cycles comparted to $2^{nd}$ cycles

## References

1 P. Roy, S. Berger and P. Schmuki, *Angew. Chem. Int. Ed.*, 2011, **50**, 2904.

2 G. G. Zhang, H. T. Huang, Y. H. Zhang, H. L. W. Chan and L. M. Zhou, *Electrochem. Commun.* 2007, **9**, 2854.

3 G. Nagasubramanian and D. H. Doughty, *J. Power Sources*, 2004, **136**, 395.

4 M. Nathan, D. Golodnitsky, V. Yufit, E. Strauss, T. Ripenbein, I. Shechtman, S. Menkin and E. Peled, *J. Microelectromech. Syst.*, 2005, **14**, 879.

5 P. L. Taberna, S. Mitra, P. Poizot, P. Simon and J.M. Tarascon, *Nat. Mater.* 2006, **5**, 567.

6 M.J. Lindsay, M.G. Blackford, D.J.Attard,V. Luca, M. Skyllas-Kazacos and C.S. Griffith, *Electrochim. Acta*, 2007, **52**. 6401.

7 H.S. Min, B. Y. Park, L. Taherabadi, C. Wang, Y. Yeh, R. Zaouk, M. J. Madou and B. Dunn, *J. Power Sources*, 2008, **178**, 795.

8 S. K. Cheah, E. Perre, M. Rooth, M. Fondell, A. Hårsta, L. Nyholm, M. Boman, J. Lu, P. Simon and K. Edström, *Nano Lett.*, 2009, **9**, 3230.

9 G. F. Ortiz, I. Hanzu, T. Djenizian, P. Lavela, J. L. Tirado and P. Knauth, *Chem. Mater.*, 2009, **21**, 63.

10 H.T. Fang, M. Liu, D.W. Wang, T. Sun, D.S. Guan, F. Li, J. Zhou, T.K. Sham and H.M. Cheng, *Nanotechnology*, 2009, **20**, 225701.

11 M. M. Shaijumon, E. Perre, B. Daffos, P.L. Taberna, J.M. Tarascon and P. Simon, *Adv. Mater.*, 2010, **22**, 4978.

12 G. F. Ortiz, I. Hanzu, P. Lavela, J. L. Tirado, P. Knauth and T. Djenizian, *J. Mater. Chem.*, 2010, **20**, 4041.

13 T. Djenizian, I. Hanzu and P. Knauth, *J. Mater. Chem.*, 2011, **21**, 9925.

14 N. A. Kyeremateng, F. Dumur, P. Knauth, B. Pecquenard and T. Djenizian, *Electrochem. Commun.* 2011, **13**, 894.

15 W. Wang, M. Tian, A. Abdulagatov, S. M. George, Y.C. Lee and R. Yang, *Nano Lett.*, 2012, **12**, 655.

16 W. Zeng, F. Zheng, R. Li, Y. Zhan, Y. Li and J. Liu, *Nanoscale*, 2012, **4**, 2760.

17 W.H. Ryu, D.H. Nam, Y.S. Ko, R.H. Kim and H.S. Kwon, *Electrochim. Acta*, 2012, **61**, 19.

18 K. Gerasopoulos, E. Pomerantseva, M. McCarthy , A. Brown , C. Wang, J. Culver and R. Ghodssi, *ACS Nano*, 2012, **6**, 6422.

19 M. Roberts, A. F. Huang, P. Johns and J. Owen, *J. Power Sources*, 2013, **224**, 250.